International Journal of Latest Engineering Research and Applications (IJLERA) ISSN: 2455-7137

Volume – 03, Issue – 04, April 2018, PP – 59-68

Group-based Sparse and Low-Rank Representation for Diagnosis of Diabetic Retinopathy

D. Ashok kumar[1], A.Sankari[2]

[1](*Department of Computer Science, Government Arts College, Trichirappalli-620 022)*

[2](*Department of Computer Science , Research Scholar, Bharathidhasan University, Trichirappalli-620 022)*

Abstract: Diabetic Retinopathy (DR) is caused by diabetes mellitus that damages the retina and leads to the vision loss. The development of automatic system for the diagnosis and grading of DR depends on the efficient detection of lesions in the retinal fundus images. Existing detection approaches suffer due to high complexity and are not feasible. To mitigate this issue, this paper presents a group-based low-rank sparse representation for the detection of DR. A Hybrid Morphological-based Scanning Window Analysis and Hit-or-Miss Transformation (HMSWA-HMT) is applied for the segmentation of retinal image. Group-based low-rank sparse representation is applied for extracting the candidate features from the segmented images. The Difference Subspace Sparse representation based Classification (DSSRC) method focuses on improving the distinguishability for the classes rather than the representation capability for the samples. The DSSRC is applied for the classification of the retinal images into normal and abnormal images. From the experimental analysis, it is observed that the proposed work yields high sensitivity, specificity and accuracy than the existing classification techniques.

Keywords: Diabetic Retinopathy, Dictionary Learning, Group-based Sparse Representation, Low-Rank Sparse Representation.

I. INTRODUCTION

Diabetic Retinopathy (DR) is one of the most common cause of vision impairment and blindness caused by Diabetes Mellitus [1]. With the increasing pervasiveness of diabetes and aging population in 2025, 333 million diabetic patients across the world will require retinal examination annually [2]. The DR can be managed efficiently using available treatments, if the disease can be diagnosed in the earlier stages. Regular eye fundus examination is required for monitoring the changes in retina[3]. Due to the limited number of ophthalmologists, there is a need for automating the screening process to reduce the burden on the ophthalmologist. The severity level is identified by grading the disease for allowing appropriate and consistent referral to the treatment centers [4].

A computer-aided diagnosis and grading system depends on the automatic detection of bright lesions such as cotton wool spots, hard and soft exudates and red lesions such as Microaneurysms (MA) and Hemorrhages (HE). MA is the earliest sign of mild Non-Proliferative DR (NPDR). MA is round-shaped intra-retinal lesion whose size ranges from 10 to 100 μm in size and color is red. The detection of MA is vital for preventing advance progression of DR[5, 6]. The MA detection algorithms are categorized as mathematical morphology [7-9], filter-based algorithms [10, 11]and supervised learning algorithms[8, 12-14]. The mathematical morphology techniques are more complex and make it difficult to execute and understand.The filter-based algorithm designs appropriate filters to match the MA.The supervised learning methods are not feasible when the training time of a large number of images is large.

In our previous work, a hybrid method for the segmentation and classification of retinal images is proposed. The significant points such as end points, bifurcations and crossing points are identified for the identification of arteriovenous nicking and diagnosis of hypertension. But, the proposed method require high time complexity than the existing classification method [15]. To overcome this issue, this paper presents a group-based low-rank sparse representation for the detection of DR. A HMSWA-HMT is applied for the segmentation of retinal image. Group-based low-rank sparse representation is applied for extracting the candidate features from the segmented images. The DSSRC method is applied for the classification of the retinal images into normal and abnormal images.

The sections in the manuscript are well-organized in the following way: Section II describes an overview of the prevalent feature extraction techniques for the diagnosis of Diabetic Retinopathy. Section III explains the proposed work including contrast enhancement and Group-based low-rank sparse representation. Section IV illustrates the comparative analysis of the proposed work with the existing classification techniques. The concluding statements are discussed in Section V.

II. EXISTING FEATURE EXTRACTION APPROACHES

Franklin and Rajan [16] presented a technique to detect and analyze the vascular structures in retinal images for the early detection of DR. A Multilayer Perceptron Neural Network (MPNN) is applied for segmenting the retinal blood vessel. The severity and progressive stages of the disease are identified using the retinal blood vessel morphology. The proposed method achieved high segmentation accuracy of about 95.03% while evaluated on the DRIVE database. Welikala et al. [17] described an automated method for detecting new vessels in the retinal images to detect Proliferative DR (PDR). Local morphology features are obtained from each binary vessel map to produce double separate feature sets. A Support Vector Machine (SVM) classifier is applied for the independent classification of each feature set. The sensitivity and specificity of the proposed method are 86.2% and 94.4% on a per patch basis and 100% and 90% on a per image basis respectively. Mann and Kaur[18] applied Artificial Neural Network (ANN)for the segmentation of retinal blood vessel. The features such as Gabor, moment invariant-based, intensity, vesselness and gray-level based features are extracted to compute the feature vector. The ANN achieved better accuracy, sensitivity, specificity and Receiver-Operating Curve (ROC) than the existing technique.

Vanithamani and Christina [19] proposed an approach for detecting the exudates to diagnose the DR. The exudates are segmented by removing the blood vessels and Optic Disc(OD) from the retinal fundus images. The Grey Level Co-occurrence Matrix (GLCM) features are extracted from the image and used for training and testing the classifiers. This automated system can efficiently filter out the exudate images and reduce the burden on ophthalmologist in classifying the exudate images manually. Seoud et al. [3]described a new method for the detection of MAs and hemorrhages by using the dynamic shape features. These features enable discrimination between the lesions and vessel segments. The proposed method achieved high sensitivity and specificity and consumed minimum computation time. Walvekar and Salunke[20] extracted features such as blood vessels, Hard Exudates (HEs) and Soft Exudates (SEs), MAs and OD for detecting the severity of DR.

Zhao et al. [21] developed a novel infinite active contour model for automatic detection of blood vessel structures. Better detection of oscillatory structures is enabled based on the boundary length of features. The intensity information and local phase based enhancement map are combined to maintain the edges of blood vessel for better segmentation performance. The proposed contour model achieved high sensitivity, specificity and accuracy for the DRIVE dataset. Kumar et al. [22] discussed about efficient approaches for localization of features and lesions in a fundus image. The features such as hemorrhages, MAs, HEs and SEs are extracted. The extracted features yield about 95% for MA, 95% sensitivity and 94% specificity for exudates identification and 97% success rate for the localization of OD. Choudhury et al. [23] proposed an approach for feature extraction using FCM and morphological methods and SVM based classification of the retinal images for the detection of DR. The features such as retinal vessel density and exudate density are applied to the SVM to classify the images into respective classes. The classification accuracy of about 97.6% is achieved. Nandy et al. [24] proposed a Gaussian Mixture Model (GMM)-based feature extraction with the refinement framework to obtain the subsequent distribution of the lesions for each retinal image. The extracted features are applied to the SVM classifier, for the efficient diagnosis of DR. The proposed framework achieved better ROC area values for different databases.

Nivetha et al. [25] proposed a new method for finding the exudates patches from the retinal blood vessels during DR treatment. The GLCM features are extracted and features are processed using Probabilistic Neural Network (PNN) classifier. Morphological operations are applied to the abnormal image for extracting blood vessels and FCM is applied to detect the exudates in the blood vessels. Sisodia et al.[26] applied preprocessing and feature extraction method for the detection of DR using machine learning techniques. Totally, 14 features are extracted from the normal and diabetic retinal fundus image. Among them, seven features such as exudate area, blood vessel area, bifurcation point count, Shannon Entropy, optic distance, hemorrhage area and MA area are extracted to identify the normal and abnormal image. Saha et al. [27] proposed a new diagnosis system for the detection of bright and dark lesions using Naïve Bayes and SVM classifier. The detection of MAs and blood vessel is eliminated by using the improved machine learning algorithms. Cortés-Ancos et al. [28]integrated MA extraction method and classification system for detecting the diabetic retinopathy. The methodology detected the low contrast MAs with lower false positive rates. Lachure et al. [29] proposed a system for detecting retinal micro-aneurysms and exudates for automatic screening of diabetic retinopathy using SVM and KNN classifier. The morphological operations are performed to find MA and features such as GLCM and structural features are extracted for classification of disease severity as normal, moderate and severe.

III. PROPOSED WORK

Initially, the input retinal images are preprocessed for enhancing the image quality. The HMSWA-HMT is applied for the segmentation of retinal image. The morphological operators are applied to minimize the

noise or enhance the image. The SWA method provides better localization irrespective of the complex disorder patterns in the image. The HMT detects the significant points such as bifurcations points, ridge and vessel ends that are able to define the vascular skeleton. Group-based low-rank sparse representation is applied for extracting the candidate features from the segmented images. The DSSRC method focuses on improving the distinguishability for the classes rather than the representation capability for the samples. The DSSRC is applied for the classification of the retinal images into normal and abnormal images. Fig.1 illustrates the overall flow diagram of the proposed work.

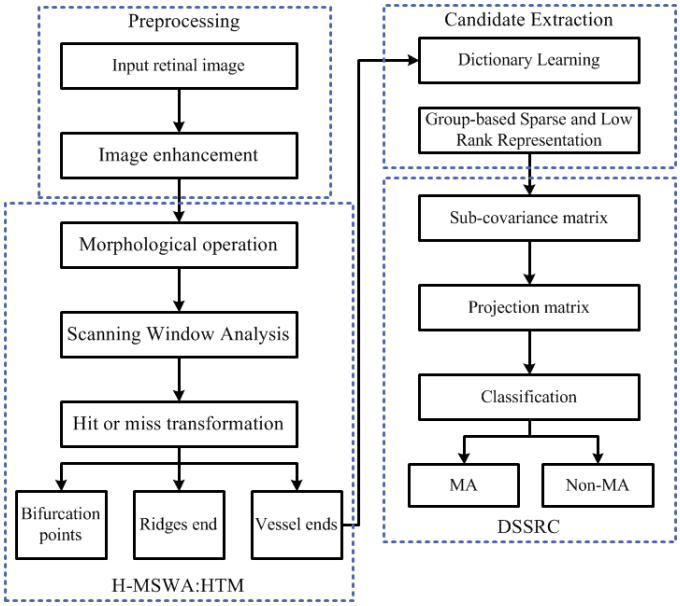

Fig.1 Overall flow diagram of proposed work

a. Contrast Enhancement

The retinal fundus images acquired at the standard ophthalmological examinations suffer from noisy, poor contrast and illumination variations. There arises a need for image preprocessing to improve the contrast and sharpness and reduce the noise and illumination variations for enabling effective analysis of the fundus images. The main objective of the preprocessing technique is to remove the noise and dark abnormalities in the retinal images. The Red, Green and Blue (RGB)color space is transformed into Lab color space to prevent the problems related with the use of gray scale methods to each color component due to the high correlation between these components. The Contrast Limited Adaptive Histogram Equalization (CLAHE) [30]is applied for improving the contrast in the retinal images.

It computes several histograms corresponding to an individual fragment of the retinal image and applies them to redistribute the intensity values of the image. Therefore, it is significant to enhance the local contrast of the image and provide detailed information about the exudates. The contrast of these regions is improved by converting each pixel using a transformation function proportional to the Cumulative Distribution Function (CDF) of the neighborhood pixels. CLAHE is applied for improving the contrast and enhancing the separability between the exudates and the background in the retinal images. This also enables the visibility of hidden features in the retinal images by smoothing the distribution of the grey values [31].

b. Feature Extraction

To classify the image into the candidate regions of exudates or non-exudates classes, it should be represented using the significant features to achieve the best class separability. To select an adequate set of features, the exudates are distinguished from other retinal lesions or structures. In our work, group-based low-rank sparse representation is applied for extracting the candidate features from the segmented images.

Group-based low-rank sparse representation

In the dictionary learning algorithm, the images are denoted as a linear combination of atoms in a dictionary 'D'. The sparse representation of the input image 'y' is learned through the optimization problem[32]

$$\hat{x} = \arg\min_x \|x\|_o \; subject\ to\ y = Dx \qquad (1)$$

Where $\|x\|_o$ denotes l_o norm that provides the number of non-zero entries in the vector 'x'. K-SVD algorithm is one of the methods for learning a dictionary from the training samples. K-means clustering is considered as a method for sparse representation to find the best possible codes for representing 'y' using the nearest neighbor method

$\arg\min_{D,X}\|Y - DX\|_F^2 \ such\ that\ \forall_i, \|x_i\|_o = 0$ (2)

The sparse representation $\|x\|_o = 1$ applies K-means algorithm to ensure one atom in the dictionary. As the K-SVD algorithm intends to achieve linear combinations of atoms, the constraint is updated in such a way that $x_i > 1 \text{and} x_i < T_o$,

$\arg\min_{D,X}\|Y - DX\|_F^2 \ such\ that\ \forall_i, \|x_i\|_o \leq T$ (3)

Where $X = [x_1, \dots, x_N], x_i \epsilon R^k$ are sparse codes of 'N' input images. $D = [d_1, \dots, d_k], d_i \epsilon R^n$ and T restricts the input to require less than T items in its decomposition. 'k' denotes the number of atoms in the learnt dictionary and 'n' indicates the number of samples. This equation is solved for learning both the sparse codes and dictionary alternatively and iteratively. The sparse representation of the input image is obtained as the result.

The Low Rank Representation (LRR) is used for finding the LRR of the data using a given dictionary. It can recover the data from multiple subspaces and acquire the global structure of data. The objective function of Group-based Sparse and Low-Rank (GSLR) representation is expressed as

$\min_{D,Z} \frac{1}{2}\|X - DZ\|_F^2 + \lambda_1 \sum_{i=1}^n w_{\mathcal{G}_i}\left\|Z_{\mathcal{G}_i}\right\|_* + \lambda_2 \sum_{i=1}^n w_{\mathcal{G}_i}\left\|Z_{\mathcal{G}_i}\right\|_1$ (4)

Such that $Z \geq 0, \forall_i \|d_i\|_2 \leq 1, d_i \geq 0$

Where $X = [x_1, x_2, \dots, x_N]$ is a matrix comprising members of $\mathcal{X}$, $x_i \in \mathcal{X}, where\ i = 1, 2, \dots, N$. 'Z' and 'D' denote the representation matrix with the group-based sparse and low-rank regularization and the dictionary to be learned. $Z_{\mathcal{G}_i}$ refers to the i[th] group of Z, d_i denotes the i[th] column of D, λ_1 and λ_2 are the parameters that balance three terms in the objective function. $w_{\mathcal{G}_i}$ represents the regularization parameter for the i[th] group. $w_{\mathcal{G}_i} = 10\sqrt{|\mathcal{G}_i|}, where\ i = 1, 2, \dots, n$ with spatial groups $\mathcal{G}_i$. d_i represents the i[th] column of D, $\|\cdot\|_F$ and $\|\cdot\|_1$ denote the Frobenius norm and the l_1 norm of the matrix. $\|\cdot\|_*$ represents the nuclear norm of a matrix, i.e., the sum of singular values of matrix.The optimal representation matrix 'Z' is computed for a dictionary 'D' and the dictionary is solved with fixed Z.

1. Optimization of 'Z'

The representation matrix 'Z' is solved with the current dictionary 'D'. The optimization problem is modeled by

$\min_{D,Z} \frac{1}{2}\|X - DZ\|_F^2 + \lambda_1 \sum_{i=1}^n w_{\mathcal{G}_i}\left\|Z_{\mathcal{G}_i}\right\|_* + \lambda_2 \sum_{i=1}^n w_{\mathcal{G}_i}\left\|Z_{\mathcal{G}_i}\right\|_1$ (5)

Such that $Z \geq 0$

The objective function is separable with various spatial groups $\{\mathcal{G}_1, \mathcal{G}_2, \dots, \mathcal{G}_n\}$. Hence, Z can be solved for each $Z_{\mathcal{G}_i}$ independently. Without the generality loss, $Z_{\mathcal{G}_i}$ is simply expressed as Z_g with $g \subset \{\mathcal{G}_1, \mathcal{G}_2, \dots, \mathcal{G}_n\}$. The subproblem yields

$\min_Z \frac{1}{2}\left\|X_g - DZ_g\right\|_F^2 + \beta_1\left\|Z_g\right\|_* + \beta_2\left\|Z_g\right\|_1$ (6)

Such that $Z_g \geq 0$

Where X_g derives from the group 'g' of X. The above equation comprises reconstruction error, low-rank representation and sparsity of Z_g, $\beta_1 = \lambda_1 w_{\mathcal{G}_i}$ and $\beta_2 = \lambda_2 w_{\mathcal{G}_i}$ reflect the tradeoff among these three components.

Two auxiliary matrices 'E' and 'W' are added. The problem is reformulated as

$\min_Z \frac{1}{2}\|E\|_F^2 + \beta_1\left\|Z_g\right\|_* + \beta_2\|W\|_1$ (7)

$such\ that\ E = X_g - DZ_g, W = Z_g, W \geq 0$

Hence, the augmented Lagrangian function is expressed as

$\mathcal{L}(Z_g, W, E, Y_1, Y_2, \mu) = \frac{1}{2}\|E\|_F^2 + \beta_1\left\|Z_g\right\|_* + \beta_2\|W\|_1 + \boldsymbol{Q}(Z_g, W, E, Y_1, Y_2, \mu) - \frac{1}{2\mu}(\|Y_1\|_F^2 + \|Y_2\|_F^2)$

Where $\mu > 0$ denotes the penalty parameter, Y_1 and Y_2 are matrices of Lagrangian multipliers, $tr(\cdot)$ denotes the trace of a matrix and $\boldsymbol{Q}(Z_g, W, E, Y_1, Y_2, \mu) = \frac{\mu}{2}\left(\left\|X_g - DZ_g - E + \frac{Y_1}{\mu}\right\|_F^2 + \left\|Z_g - W + \frac{Y_2}{\mu}\right\|_F^2\right)$.

The $\boldsymbol{Q}$ is quadraticand approximated by its first order approximation while adding a proximal term. The above equation is unconstrained and minimized by updating the variables Z_g, W and E simultaneously. At this point, the $(k+1)^{\text{th}} Z_g$, W and E is evaluated as

$$Z_g^{k+1} = \mathcal{D}_{\frac{\beta_1}{\mu^k \eta_1}}\left(Z_g^k + \frac{1}{\eta_1}\left[D^T\left(X_g - DZ_g^k - E^k + \frac{Y_1^k}{\mu^k}\right) - \left(Z_g^k - W^k + \frac{Y_2^k}{\mu^k}\right)\right]\right) \quad (8)$$

$$W^{k+1} = \max\left[S_{\frac{\beta_2}{\mu^k}}\left(Z_g^{k+1} + \frac{Y_2^k}{\mu^k}\right), 0\right] \quad (9)$$

$$E^{k+1} = \frac{\mu^k}{1+\mu^k}\left(X - DZ^{k+1} + \frac{Y_1^k}{\mu^k}\right) \quad (10)$$

Where $\nabla_{Z_g}\boldsymbol{Q}$represents the partial differential of Q with respect to Z_g, $\eta_1 = \|D\|_2^2, \mathcal{D}_{\frac{\beta_1}{\mu^k \eta_1}}$ denotes singular value thresholding operator. Let $\mathcal{C}_1 = Z_g^k + \frac{1}{\eta_1}\left[D^T\left(X_g - DZ_g^k - E^k + \frac{Y_1^k}{\mu^k}\right) - \left(Z_g^k - W^k + \frac{Y_2^k}{\mu^k}\right)\right]$, the rank of the matrix $\mathcal{C}_1$ be r.

$(\cdot)_+ = \max(\cdot, 0)$, the singular value decomposition of $\mathcal{C}_1$ be

$\mathcal{C}_1 = U \sum V^T, \sum = diag(\{\pi_i\}_{1 \le i \le r})$

Then, Z_g^{k+1} satisfies

$$Z_g^{k+1} = U\ diag\left(\left\{\left(\pi_i - \frac{\beta_1}{\mu^k \eta_1}\right)_+\right\}_{1 \le i \le r}\right)V^T \quad (11)$$

Where, $S_{\frac{\beta_2}{\mu^k}}$ shrinkage operator is defined as

$$S_{\frac{\beta_2}{\mu^k}}(\cdot) = sign(\cdot)\max\left(0, |\cdot| - \frac{\beta_2}{\mu^k}\right)$$

2. Optimization of 'D'

In the dictionary update step, Z is fixed and 'D' is optimized by solving

$$\min_D \frac{1}{2}\|X - DZ\|_F^2\ such\ that\ \forall i \|d_i\|_2 \le 1, d_i \ge 0 \quad (12)$$

That is quadratic with respect to the dictionary. The dictionary atoms d_i with larger than the unit norm are projected inside the non-negative than a unit l_2 ball. When the gradient of the objective function equals zero,

$$D = XZ^T(ZZ^T)^{-1} \quad (13)$$

The above equation suffer from the computation of inverse of ZZ^T, the dictionary atoms are updated iteratively. Let $R_i = X - \sum_{j \ne i} d_j Z_T^{jT}$, where Z_T^j represents the j[th] row of Z in the column form. The objective function of the i[th] atom yields $\frac{1}{2}\left\|R_i - d_i Z_T^{iT}\right\|_F^2$. The objective function is rearranged as

$$\min_{d_i} \frac{1}{2}\left\|d_i - \frac{R_i Z_T^i}{\|Z_T^i\|_2^2}\right\|_2^2\ such\ that\ \|d_i\|_2 \le 1, d_i \ge 0 \quad (14)$$

Whose solution is

$$d_i = proj_{l_2^+}\left(\frac{R_i Z_T^i}{\|Z_T^i\|_2^2}\right) \quad (15)$$

Where $proj_{l_2^+}(\cdot)$ denotes the projection inside the non-negative orthant of a unit l_2 ball [33].

In the dictionary learning process, Z and D are updated alternately. The iteration of the algorithm stops, when the relative error of two successive objective functions is less than the tolerance.

Input: The matrix 'X' and parameters $\lambda_1, \lambda_2\ and\ w_{\mathcal{G}_i}$

Output: Z and D

Step 1: Initialize D^0 and $k = 0$

Step 2: while Convergence is not attained do

Step 3: Solve $Z^{k+1}, W^{k+1}, E^{k+1}$ with respect to D^k

Step 4: Update D^{k+1} with fixed $Z^{k+1}, W^{k+1}, E^{k+1}$ by solving eqn (12)

Step 5: Update 'k' by $k = k + 1$

Step 6: end while

IV. PERFORMANCE ANALYSIS

The experimental analysis is carried out using the Matlab software. The proposed work is compared with Careera et al. [34].

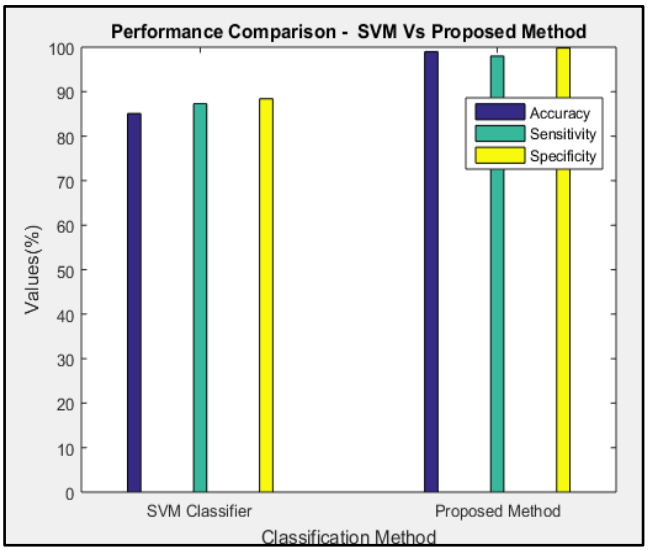

Fig.2 Accuracy, Sensitivity and Specificity analysis of the proposed work and SVM classifier

Fig.2 illustrates the accuracy, sensitivity and specificity analysis of the proposed work and SVM classifier. The SVM classifier yields sensitivity, specificity and accuracy of 85.1%, 87.3% and 88.4% respectively. The proposed work achieves high sensitivity, specificity and accuracy of about 99%, 98% and 99.8%respectively. Fig.3 depicts the accuracy, sensitivity and specificity analysis of the proposed work and DT classifier. The Decision Tree (DT) classifier yields sensitivity, specificity and accuracy of 92%, 86.6% and 97.4% respectively. The proposed work achieves high sensitivity, specificity and accuracy of about 99%, 98% and 99.8% respectively. The proposed method is compared with Sanchez et al. [35], Agurto et al. [36], Antal et al [37], Barriga et al. [38], DREAM [15] and HM-SPCA and evaluated using the MESSIDOR dataset [39]. Fig.4 depicts the comparative analysis of the sensitivity, accuracy rate and specificity for different image classification methods. The proposed approach yields maximum sensitivity, specificity and accuracy rate than the existing classification methods. Due to the extraction of the optimal features, the normal and abnormal images are classified efficiently. This facilitates the efficient diagnosis of the DR.

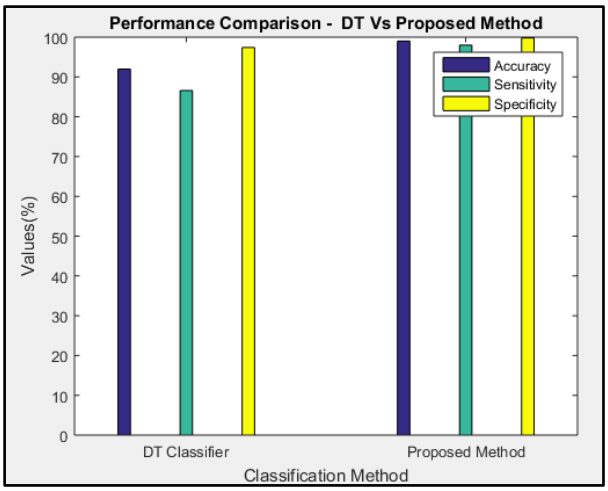

Fig.3 Accuracy, Sensitivity and Specificity analysis of the proposed work and DT classifier

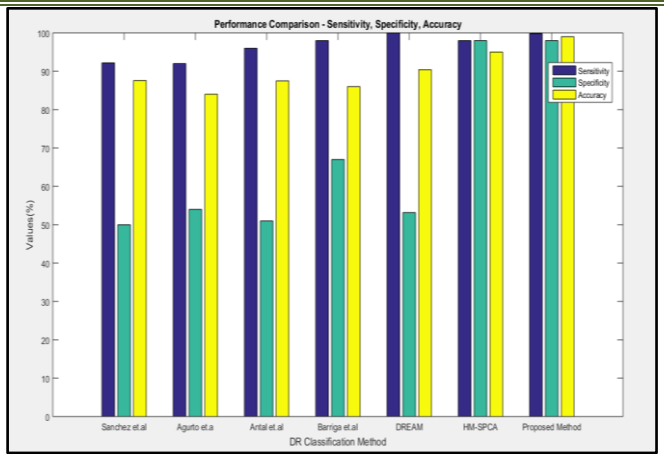

Fig.4 Accuracy, Sensitivity and Specificity analysis for different classification methods

The proposed method is compared with the retinal feature extraction approach [40]. Fig.5 shows the healthy image detection analysis. Fig.6 illustrates the Glaucoma image detection and Fig.7 presents the DR image detection. In the retinal image database, there are 25 healthy images, 15 Glaucoma images and DR images. Existing feature extraction method has extracted 25 healthy images, 14 Glaucoma images and 13 DR images. The existing method achieved accuracy of about 100%, 93.33% and 80% for the extraction of healthy images, Glaucoma images and DR images respectively. Our proposed method has successfully extracted 25 healthy images, 14 Glaucoma images and 14 DR images. The proposed method achieved accuracy of about 100%, 100% and 93.33% for the extraction of healthy images, Glaucoma images and DR images respectively.

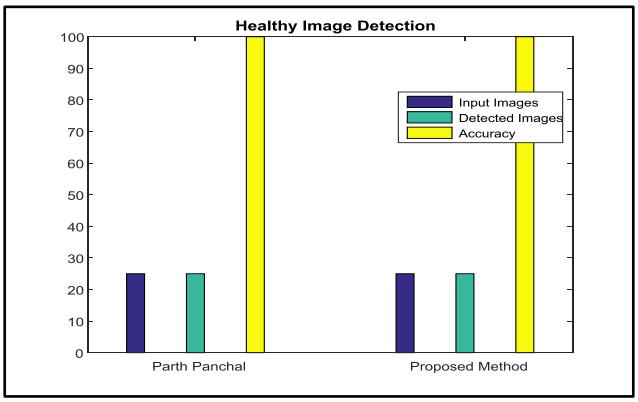

Fig.5 Healthy image detection

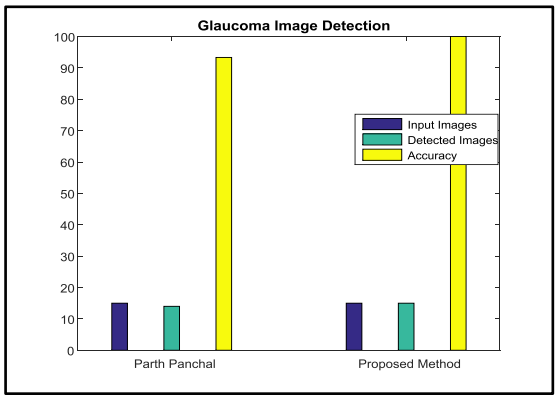

Fig.6 Glaucoma Image detection

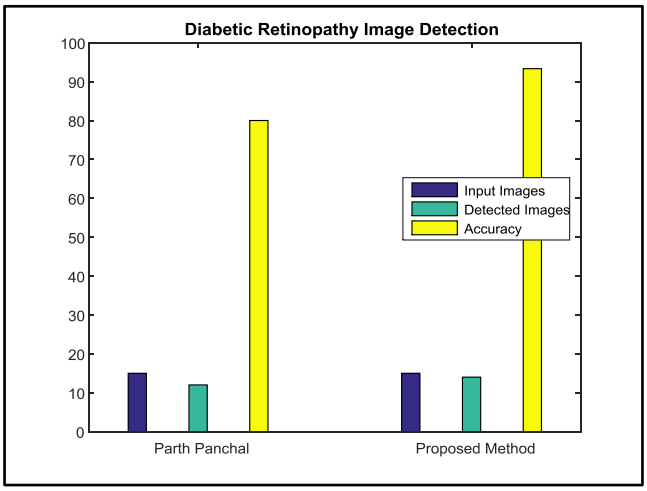

Fig.7 DR image detection

V. CONCLUSION

Dictionary Learning is applied for learning the MA and non-MA dictionaries from the sample MA and non-MA objects. Then, these dictionaries are used for representing and classifying the MA candidates using group-based low rank sparse representation. The dictionary learning with group-based sparse and low-rank regularizations makes the pixels that belong to the same group to share a common active set of atoms from the dictionary. The group-based sparse and low-rank regularizations are capable of capturing both local and global structure of the image and facilitate the integration of spatial information into the classification task. The proposed work yields high sensitivity, specificity and accuracy than the existing classification techniques. From the experimental results, it can be concluded that the proposed method is effective for MA detection, and a vital tool in the DR diagnosis.

REFERENCES

[1] N. Cheung, P. Mitchell, and T. Y. Wong, "Diabetic retinopathy," *Lancet*, vol. 376, pp. 124-136, 2010.

[2] I. D. Federation, "IDF diabetes atlas," *Brussels: International Diabetes Federation*, 2013.

[3] L. Seoud, T. Hurtut, J. Chelbi, F. Cheriet, and J. P. Langlois, "Red lesion detection using dynamic shape features for diabetic retinopathy screening," *IEEE transactions on medical imaging*, vol. 35, pp. 1116-1126, 2016.

[4] C. Wilkinson, F. L. Ferris, R. E. Klein, P. P. Lee, C. D. Agardh, M. Davis, *et al.*, "Proposed international clinical diabetic retinopathy and diabetic macular edema disease severity scales," *Ophthalmology*, vol. 110, pp. 1677-1682, 2003.

[5] A. K. Sjølie, R. Klein, M. Porta, T. Orchard, J. Fuller, H. Parving, *et al.*, "Retinal microaneurysm count predicts progression and regression of diabetic retinopathy. Post-hoc results from the DIRECT Programme," *Diabetic Medicine*, vol. 28, pp. 345-351, 2011.

[6] W. L. Yun, U. R. Acharya, Y. V. Venkatesh, C. Chee, L. C. Min, and E. Y. K. Ng, "Identification of different stages of diabetic retinopathy using retinal optical images," *Information sciences*, vol. 178, pp. 106-121, 2008.

[7] T. P. Karnowski, V. P. Govindasamy, K. W. Tobin, E. Chaum, and M. Abramoff, "Retina lesion and microaneurysm segmentation using morphological reconstruction methods with ground-truth data," in *30th Annual International Conference of the IEEE Engineering in Medicine and Biology Society, 2008. EMBS 2008.*, 2008, pp. 5433-5436.

[8] M. Niemeijer, B. Van Ginneken, J. Staal, M. S. Suttorp-Schulten, and M. D. Abràmoff, "Automatic detection of red lesions in digital color fundus photographs," *IEEE Transactions on medical imaging*, vol. 24, pp. 584-592, 2005.

[9] T. Spencer, J. A. Olson, K. C. McHardy, P. F. Sharp, and J. V. Forrester, "An image-processing strategy for the segmentation and quantification of microaneurysms in fluorescein angiograms of the ocular fundus," *Computers and biomedical research*, vol. 29, pp. 284-302, 1996.

[10] M. Niemeijer, B. Van Ginneken, M. J. Cree, A. Mizutani, G. Quellec, C. I. Sánchez, *et al.*, "Retinopathy online challenge: automatic detection of microaneurysms in digital color fundus photographs," *IEEE transactions on medical imaging*, vol. 29, pp. 185-195, 2010.

[11] G. Quellec, M. Lamard, P. M. Josselin, G. Cazuguel, B. Cochener, and C. Roux, "Optimal wavelet transform for the detection of microaneurysms in retina photographs," *IEEE Transactions on Medical Imaging*, vol. 27, pp. 1230-1241, 2008.

[12] M. García, C. I. Sánchez, M. I. Lopez, A. Diez, and R. Hornero, "Automatic detection of red lesions in retinal images using a multilayer perceptron neural network," in *Engineering in Medicine and Biology Society, 2008. EMBS 2008. 30th Annual International Conference of the IEEE*, 2008, pp. 5425-5428.

[13] G. Gardner, D. Keating, T. H. Williamson, and A. T. Elliott, "Automatic detection of diabetic retinopathy using an artificial neural network: a screening tool," *British journal of Ophthalmology*, vol. 80, pp. 940-944, 1996.

[14] G. B. Kande, T. S. Savithri, P. V. Subbaiah, and M. Tagore, "Detection of red lesions in digital fundus images," in *Biomedical Imaging: From Nano to Macro, 2009. ISBI'09. IEEE International Symposium on*, 2009, pp. 558-561.

[15] S. Roychowdhury, D. D. Koozekanani, and K. K. Parhi, "DREAM: diabetic retinopathy analysis using machine learning," *IEEE journal of biomedical and health informatics*, vol. 18, pp. 1717-1728, 2014.

[16] S. W. Franklin and S. E. Rajan, "Computerized screening of diabetic retinopathy employing blood vessel segmentation in retinal images," *biocybernetics and biomedical engineering*, vol. 34, pp. 117-124, 2014.

[17] R. Welikala, J. Dehmeshki, A. Hoppe, V. Tah, S. Mann, T. H. Williamson, *et al.*, "Automated detection of proliferative diabetic retinopathy using a modified line operator and dual classification," *Computer methods and programs in biomedicine*, vol. 114, pp. 247-261, 2014.

[18] K. S. Mann and S. Kaur, "Segmentation of retinal blood vessels using artificial neural networks for early detection of diabetic retinopathy," in *AIP Conference Proceedings*, 2017, p. 020026.

[19] R. Vanithamani and R. R. Christina, "Exudates in Detection and Classification of Diabetic Retinopathy," in *International Conference on Soft Computing and Pattern Recognition*, 2016, pp. 252-261.

[20] M. Walvekar and G. Salunke, "Detection of diabetic retinopathy with feature extraction using image processing," *international journal of emerging technology and advanced engineering*, vol. 5, pp. 133-7, 2015.

[21] Y. Zhao, L. Rada, K. Chen, S. P. Harding, and Y. Zheng, "Automated vessel segmentation using infinite perimeter active contour model with hybrid region information with application to retinal images," *IEEE transactions on medical imaging*, vol. 34, pp. 1797-1807, 2015.

[22] S. ManojKumar, R. Manjunath, and H. Sheshadri, "Feature extraction from the fundus images for the diagnosis of diabetic retinopathy," in *International Conference on Emerging Research in Electronics, Computer Science and Technology (ICERECT)*, 2015, pp. 240-245.

[23] S. Choudhury, S. Bandyopadhyay, S. Latib, D. Kole, and C. Giri, "Fuzzy C means based feature extraction and classification of diabetic retinopathy using support vector machines," in *Communication and Signal Processing (ICCSP), 2016 International Conference on*, 2016, pp. 1520-1525.

[24] J. Nandy, W. Hsu, and M. L. Lee, "An incremental feature extraction framework for referable diabetic retinopathy detection," in *IEEE 28th International Conference on Tools with Artificial Intelligence (ICTAI)*, 2016, pp. 908-912.

[25] C. Nivetha, S. Sumathi, and M. Chandrasekaran, "Retinal blood vessels extraction and detection of exudates using wavelet transform and pnn approach for the assessment of diabetic retinopathy," in *Communication and Signal Processing (ICCSP), 2017 International Conference on*, 2017, pp. 1962-1966.

[26] D. S. Sisodia, S. Nair, and P. Khobragade, "Diabetic Retinal Fundus Images: Preprocessing and Feature Extraction for Early Detection of Diabetic Retinopathy," *Biomedical and Pharmacology Journal*, vol. 10, pp. 615-626, 2017.

[27] R. Saha, A. R. Chowdhury, and S. Banerjee, "Diabetic retinopathy related lesions detection and classification using machine learning technology," in *International Conference on Artificial Intelligence and Soft Computing*, 2016, pp. 734-745.

[28] E. Cortés-Ancos, M. E. Gegúndez-Arias, and D. Marin, "Microaneurysm Candidate Extraction Methodology in Retinal Images for the Integration into Classification-Based Detection Systems," in *International Conference on Bioinformatics and Biomedical Engineering*, 2017, pp. 376-384.

[29] J. Lachure, A. Deorankar, S. Lachure, S. Gupta, and R. Jadhav, "Diabetic Retinopathy using morphological operations and machine learning," in *IEEE International Advance Computing Conference (IACC), 2015*, 2015, pp. 617-622.

[30] E. Clahe, "Contrast Limited Adaptive Histogram Equalization Clahe."

[31] S. W. Franklin and S. E. Rajan, "Diagnosis of diabetic retinopathy by employing image processing technique to detect exudates in retinal images," *IET Image processing*, vol. 8, pp. 601-609, 2014.

[32] Z. He, L. Liu, S. Zhou, and Y. Shen, "Learning group-based sparse and low-rank representation for hyperspectral image classification," *Pattern Recognition*, vol. 60, pp. 1041-1056, 2016.

[33] A. Soltani-Farani, H. R. Rabiee, and S. A. Hosseini, "Spatial-aware dictionary learning for hyperspectral image classification," *IEEE Transactions on geoscience and remote sensing*, vol. 53, pp. 527-541, 2015.

[34] E. V. Carrera, A. González, and R. Carrera, "Automated detection of diabetic retinopathy using SVM," in *Electronics, Electrical Engineering and Computing (INTERCON), 2017 IEEE XXIV International Conference on*, 2017, pp. 1-4.

[35] C. I. Sánchez, M. Niemeijer, A. V. Dumitrescu, M. S. Suttorp-Schulten, M. D. Abramoff, and B. van Ginneken, "Evaluation of a computer-aided diagnosis system for diabetic retinopathy screening on public data," *Investigative ophthalmology & visual science*, vol. 52, pp. 4866-4871, 2011.

[36] C. Agurto, V. Murray, E. Barriga, S. Murillo, M. Pattichis, H. Davis, *et al.*, "Multiscale AM-FM methods for diabetic retinopathy lesion detection," *IEEE transactions on medical imaging*, vol. 29, pp. 502-512, 2010.

[37] B. Antal and A. Hajdu, "An ensemble-based system for microaneurysm detection and diabetic retinopathy grading," *IEEE transactions on biomedical engineering*, vol. 59, pp. 1720-1726, 2012.

[38] E. S. Barriga, V. Murray, C. Agurto, M. Pattichis, W. Bauman, G. Zamora, *et al.*, "Automatic system for diabetic retinopathy screening based on AM-FM, partial least squares, and support vector machines," in *Biomedical Imaging: From Nano to Macro, 2010 IEEE International Symposium on*, 2010, pp. 1349-1352.

[39] A. Aazami, S. Ghandeharizadeh, and T. Helmi, "Near Optimal Number of Replicas for Continuous Media in Ad-hoc Networks of Wireless Devices," in *Multimedia Information Systems*, 2004, pp. 40-49.

[40] P. Panchal, R. Bhojani, and T. Panchal, "An Algorithm for Retinal Feature Extraction using Hybrid Approach," *Procedia Computer Science*, vol. 79, pp. 61-68, 2016.

